Tetrahedron 65 (2009) 3496–3501

Contents lists available at ScienceDirect

Tetrahedron

journal homepage: www.elsevier.com/locate/tet

Photoresponsive organogels: an amino acid-based dendron functionalized with *p*-nitrocinnamate

Gui-Chao Kuang [a], Yan Ji [a], Xin-Ru Jia [a,*], Yan Li [a], Er-Qiang Chen [a], Zheng-Xiang Zhang [a], Yen Wei [b,*]

[a] Beijing National Laboratory for Molecular Sciences, Key Laboratory of Polymer Chemistry and Physics of the Ministry of Education, College of Chemistry and Molecular Engineering, Peking University, Beijing, China
[b] Department of Chemistry, Drexel University, Philadelphia, USA

ARTICLE INFO

Article history:
Received 2 September 2008
Received in revised form 12 February 2009
Accepted 13 February 2009
Available online 25 February 2009

Keywords:
Photoresponsive
Organogel
Self-assembly
Natural amino acid
Dendron

ABSTRACT

An amino acid-based dendron **1**, synthesized and focally functionalized with *p*-nitrocinnamate, can self-assemble into fibrous network in common organic solvents at low concentration. The most remarkable character of the gel from **1** is photoresponse besides thermo-reversible response. Upon irradiation with UV light at 365 nm, gel to sol transition occurred resulting from the photodimerization of *p*-nitrocinnamate groups. On the other hand, when the obtained solution was further exposed to short wavelength of UV light at 254 nm, the gel re-formed because of the photocleavage reaction.

1. Introduction

Stimuli-responsive materials, such as organogels from low molecular weight organogelators, (LMOGs, Mw≤3000), remain an exciting field due to their potential applications, including sensor materials, chemical valves, catalysis, mechanical transducers, controlled release systems, and artificial muscles for the biomedical purpose. Apart from response to light,[1] temperature,[2] pH,[3] coordination function,[4] redox stimuli,[5] and even ultrasound[6] have become the novel paths to reversibly control the morphology of assemblies via weak interactions. In the past few years, covalently combining functional groups in an organogelator have attracted much attention. Several groups have presented their works by employing photochromic molecules as building blocks to afford smart gelators, such as the most widely used azobenzene systems,[7] stilbene-containing surfactants,[8] bisthienylethene derivatives,[9] butadiene-containing compounds,[10] and bis(phenylalanine) maleic acid,[11] which all displayed sol–gel phase transition with UV light as a switching trigger. Recently, Shimizu et al. reported a thymine-containing bolaamphiphiles that showed a reversible photochemical conversion of self-assembled helical nanofibers.[12] Shinkai et al. and Zhu et al. separately described the photoresponsive behavior of organogelators derived from anthracene derivatives.[13] In our previous report, we also presented the photoreversible property of an amino acid-based dendritic gelator with an azobenzene group at the focal point.[14]

Photodimerization of cinnamate groups by ultraviolet light is one of the widely investigated photochemical reactions. The cinnamate groups proceed [2+2] cycloaddition upon irradiation with UV light at 365 nm, and the cyclobutane derivatives will undergo photocleavage reaction by irradiating with UV light of short wavelength to regenerate the monomers.[15] Nowadays, to build a cyclobutyl through [2+2] cycloaddition in simple organic systems as well as in polymers is one of the most cost-effective methods. However, research interests have been mainly focused on the photodimerization of poly(vinyl cinnamate) films and the liquid crystalline properties of cinnamate-containing compounds.[16] Only a few studies related to gel phase assembly of the cinnamate-modified compounds have been documented.[17] For example, Koshima et al. reported the coumarin-derived organogelators that showed reversible and stereoselective photodimerization with the morphology change in cyclohexane.[18] However, the reversible conversion of gel to sol and sol to gel didn't occur when it was irradiated by UV light at different wavelength. Andreopoulos et al. investigated the photoreactivity of cinnamate-functionalized polymeric hydrogel and evaluated their low toxicity utilizing the XTT viability assays.[19] Nevertheless, a dendritic gelator modified

* Corresponding authors. Tel.: +86 10 62752102; fax: +86 10 62751708 (X.-R.J.); tel.: +1 215 895 2652; fax: +1 215 895 1265 (Y.W.).
E-mail addresses: xrjia@pku.edu.cn (X.-R. Jia), weiyen@drexel.edu (Y. Wei).

0040-4020/$ – see front matter © 2009 Elsevier Ltd. All rights reserved.
doi:10.1016/j.tet.2009.02.038

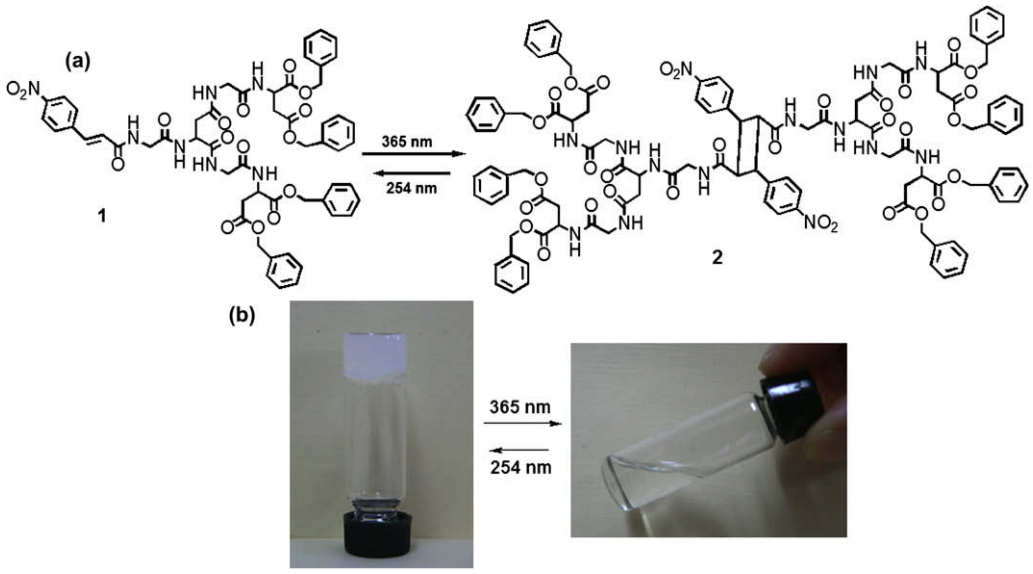

Scheme 1. (a) Schematic representation of the photoresponse of monomer **1** and dimer **2**. (b) Representative photographic images of the photoresponsive gel (left) from **1** in acetone and the solution of **2** (right) obtained from **1** after 365 nm UV-light irradiation.

with a cinnamate group that can respond to light has never been reported so far. Herein, we describe a new type of photoresponsive organogel from self-assembly of dendron **1** with glycine and aspartic acid as building blocks and a *p*-nitrocinnamate group at the focal point. Upon irradiation with UV light at 365 nm, gel to sol transition was observed, which resulted from photodimerization of *p*-nitrocinnamate groups. On the other hand, when the obtained solution was further exposed to short wavelength of UV light at 254 nm, the gel re-formed (Scheme 1).

2. Results and discussion

2.1. Organogel properties

The dendritic compound **1**, which could be easily prepared from inexpensive starting materials in 62% yield, was identified by NMR and matrix-assisted laser desorption/ionization time-of-flight (MALDI-TOF) mass-spectra, while the purity of the compound was established by elemental analysis. Compound **1** can act as an efficient LMOG. It gels organic solvents at very low concentration (usually <2%) through non-covalent forces. The solvents that can be gelled by **1** are summarized in Table 1. Of all the solvents that were tested (e.g., ethyl ester, methanol, 1,2-dichloroethane, THF, cyclohexane, acetone, etc.), acetone was gelled with a minimum concentration. Moreover, **1** also formed organogel in the mixed solvents. For example, **1** (6 mg) was first dissolved in a mixture of methanol and chloroform (0.6 mL, 1:5, v/v). With the addition of ethyl acetate (0.5 mL) and then by sonication (SY-3100 D, sonic power 150 W), the transparent solution immediately became viscous and gelled within 5 s. The gels were stable at rt for more than half a year and could be readily converted between sol and gel by heating and cooling. However, the gel was easily destroyed by mechanical agitation and not re-formed renewedly. The gelation ability of **1** in acetone was tested under various concentrations. As shown in Figure 1, the T_{gel} (the temperature of gel dropped and vanished) values, tested in a sealed tube (diameter ~1 cm), increased with the increase of concentration and reached a plateau region above 30 mg/mL.

The weak interactions, responsible for the self-assembly of **1**, including π–π stacking and hydrogen-bonding interactions, were supported by UV–vis, ^{1}H NMR and FTIR spectroscopy, respectively. The absorption peak at 309 nm was ascribed to π–π* electronic transition of the cinnamate groups in dilute solution. This peak

Table 1
Gelation behavior of **1** in the solvents at 25 °C

Solvents	1	MGC[a]
Methanol	S	—[b]
Acetone	G	3
Chloroform	G	8
THF	G	6
1,2-Dichloroethane	G	6
Ethyl ester	P	—[c]
Cyclohexane	Ins	—[c]
DMSO	S	—[b]
DMF	S	—[b]
H_2O	P	—[c]

S: solution, G: gelation, P: precipitation, Ins: insolubility.
[a] Minimum gelation concentration, mg/mL.
[b] No gelation below 100 mg/mL.
[c] Values not tested.

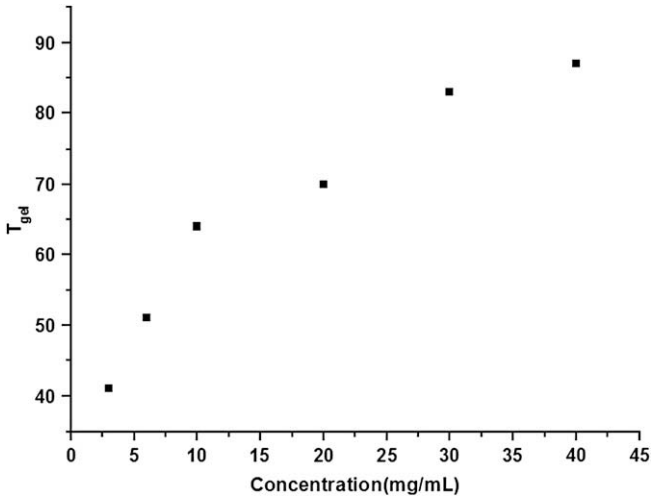

Figure 1. Plots of T_{gel} (°C) against gelator concentrations in acetone with the heating rate of 0.5 °C /min in a water bath.

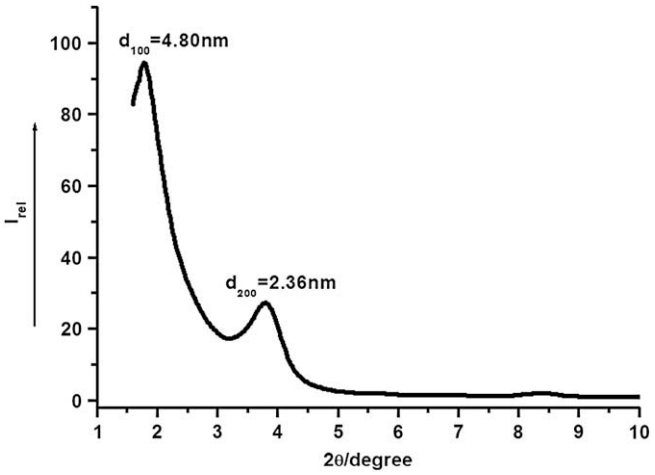

Figure 2. Powder X-ray diffraction of the xerogel of **1** in acetone.

red-shifted 17 nm and appeared at 326 nm in the gel state (see Supplementary data), indicating that the *p*-nitrocinnamate groups were packed in the *J*-aggregation.[20] As another driving force for the self-assembly, intermolecular hydrogen-bonding between the amide groups was evidenced by FTIR spectra. The N–H stretching and the amide I band presented at 3308, 1628 cm^{-1} in gel state, but these bands shifted to 3446, 1666 cm^{-1} in solution, respectively, which strongly supported the existence of the hydrogen-bonding interaction.[21] The ^{1}H NMR measurements employed in $CDCl_3$ at different temperatures (see Supplementary data) showed that the signals due to the protons of amide groups were observed at 8.03 and 7.08 ppm in the gel state at 298 K. When the temperature was increased to 313 K, the gel to sol transition occurred with the signals of the same protons shifted to 7.89 and 6.96 ppm, respectively. When the temperature was further increased to 323 K, the gel was totally destroyed. As a result, the signals were well resolved and shifted to 7.83 and 6.90 ppm. Further proof for hydrogen-bonding was that the addition of LiCl turned the gel into transparent solution, since LiCl could interact strongly with amide groups.[22]

Wide-angle X-ray diffraction (WAXD) experiments on the xerogels were performed to elucidate the possible molecular packing patterns of the gels. The XRD patterns of xerogels prepared from **1** in acetone and that in mixed solvents showed the same features (Fig. 2). In the low angle region, the corresponding scattering vector ratios followed 1:2, which indicated a lamellar structure. The long period of the lamellae is 4.8 nm. According to the basis of CPK molecular model, the size (from the focal point to the periphery) of cinnamate-functionalized dendron is estimated to be about 2.6 nm if **1** is in a fully extended state. Therefore, the *d* spacing of 4.8 nm is smaller than twice of the extended molecular size of **1**, suggesting a bilayer structure in which the cinnamate groups are partially interdigitated. Considering the dimension of stretched structure of **1**, it might be proposed that each lamellar layer consists of double building blocks of **1**; in each inner part of the lamellae, the dendrons might associate with their neighbors through hydrogen bonds; the peripheral benzyl rings are packed on the top and bottom surfaces of the lamellae; and the nitrocinnamate groups are partially packed at the center of the lamellae (Fig. 3). This packing pattern is also consistent with that of the efficient photochemical [2+2] dimerization takes place only when the cinnamate groups are aligned in a parallel manner with the distance around 3.6–4.1 Å.[23]

2.2. Photoresponsive properties

A notable character of gel from **1** is the photoresponse besides thermo-reversible response. Transmission electron microscopy (TEM), atomic force microscopy (AFM), UV–vis, ^{1}H NMR, ^{13}C NMR, MALDI-TOF MS, and reverse-phase high performance liquid chromatography (RP HPLC) were utilized to confirm the sol–gel and gel–sol transitions, which were derived from the photodimerization and photocleavage of the focal cinnamate chromophore of **1**. As expected, the gel from **1** converted to solution because of the [2+2] cycloaddition reaction induced by UV irradiation at 365 nm. Structurally, the central cyclobutane ring displayed a butterfly shape with the spacing decreasing from 4.8 nm to 3.4 nm calculated from XRD results. Consequently, it blocked the π–π stacking and hindered the hydrogen-bonding interaction of **1** resulting in the gel collapse as evidenced from the CPK model (Fig. 3). Eventually, the ring twisted the dimmer and destroyed the gel. From the FTIR measurements, the N–H stretching, the amide I and II bands are showed at 3423, 1667, and 1522 cm^{-1} in solution, which strongly indicates that non-covalent forces were destroyed (see Supplementary data). The gel could re-form after further exposed to 254 nm UV light due to regeneration of the monomer **1** by photocleavage reaction of the cyclobutane.

TEM was used to observe the morphology of the gels. As shown in Figure 4, **1** self-assembled to ramified and intertwined fibers with diameter about 25 nm and length up to several micrometers. The TEM image of xerogel from the photo-reformed gel also showed a similar morphology, wherein the fiber diameter (or width) presents a broad distribution from 5 to 25 nm (Fig. 4b). Compared with the fibrous network structure of the original gel shown in Figure 4c, the re-formed gel showed the co-existence of both intertwined fibers and amorphous structure on the fresh mica (Fig. 4d).

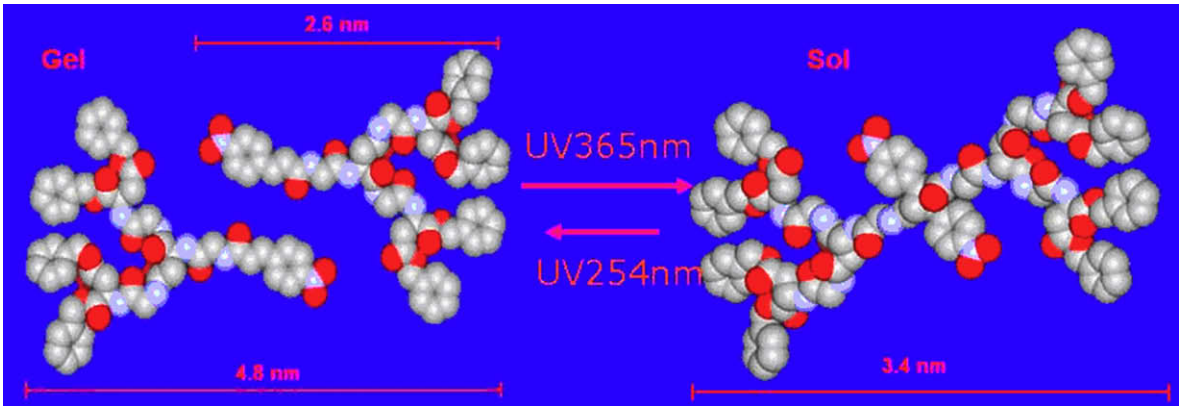

Figure 3. CPK molecular model of monomer **1** and dimer **2**.

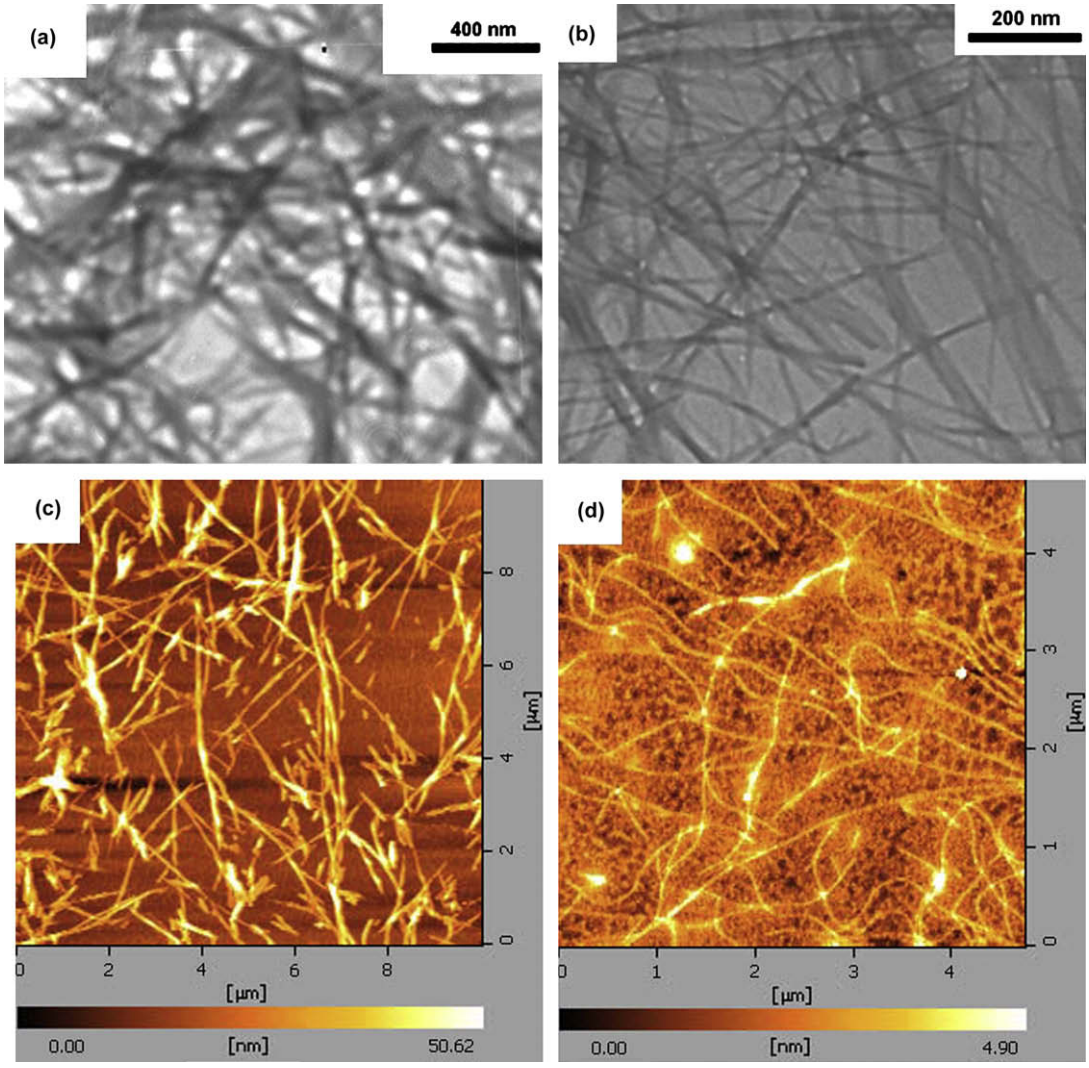

Figure 4. (a) TEM and (c) AFM images of the original xerogel from **1**. (b) TEM and (d) AFM images of re-formed gel obtained by UV irradiation at 254 nm.

The UV–vis spectra showed that the absorption peak of cinnamate groups emerged at 326 nm. It decreased continuously with time lasting and blue-shifted to 310 nm (absorption peak of the dimer) upon 365 nm irradiation, indicating the occurrence of dimerization reaction and cis–trans isomerization.[24] However, when the dimer solution was irradiated with short UV wavelength of 254 nm, the intensity of absorption band at 310 nm decreased further, became broader and red-shifted 8 nm (Fig. 5).[25] This result is consistent with the previous report of Andreopoulos' group.[19] They argued that the incomplete photocleavage reaction of the dimers might lead to the inefficient photoscissive light. In our case, it might be due to the following combined reasons: (a) photodegradation of the ester linkage in the dendritic branches due to irradiation with 254 nm UV light (several peaks appear at the low value region after 254 nm irradiation as shown in Fig. S6c, Supplementary data); (b) cinnamylidene photodegradation is facilitated by 254 nm irradiation; and (c) strongly confined photocleavage reaction because the presence of nitro group plays an important role in enhancing the rate of photo-cycloaddition reaction.[19c]

In the ^{1}H NMR spectra (Fig. 6), the signals at 6.2–6.3, 6.9–7.0 ppm and 6.6–6.8, 7.4–7.6 ppm are attributed to the *cis*- and *trans*-cinnamylidene protons, respectively. After irradiation with 365 nm UV light, the integration areas of the phenyl protons increased from

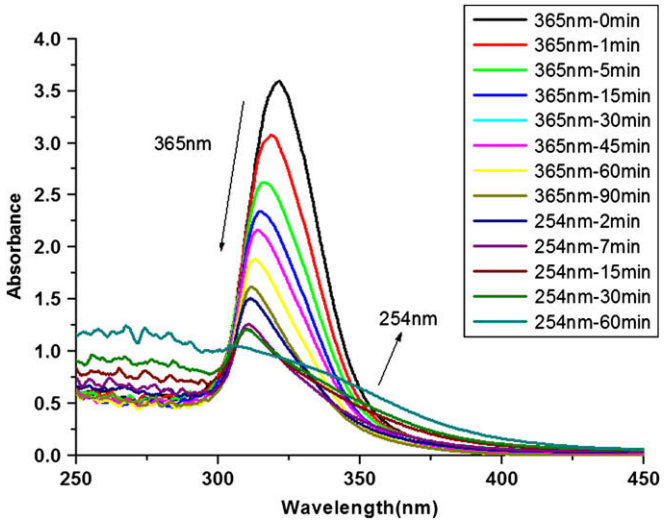

Figure 5. Absorption spectra of the gel from **1** in mixed solvents (methanol, chloroform, and ethyl acetate) and its response to UV light with different wavelength as a function of time. A 0.1 mm optical path length quartz cell with a Teflon cap was applied. The 100 W UV lamp (365 nm) and 8 W UV lamp (254 nm) were utilized with the distance kept from quartz cell 5 cm and 10 cm, respectively. Concentration: 6 mg/mL.

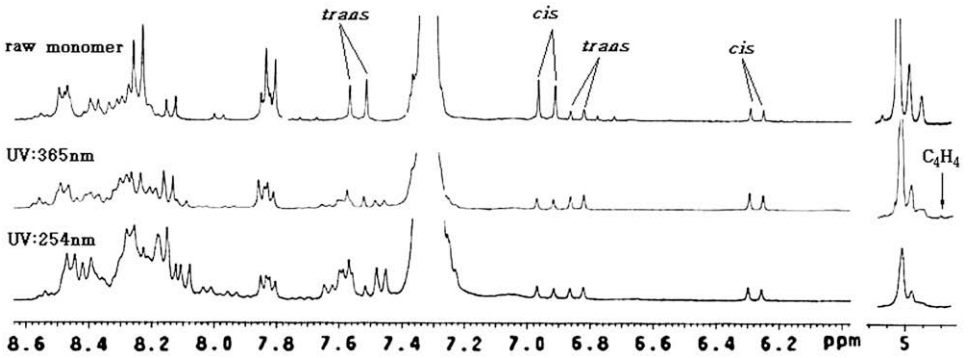

Figure 6. ^{1}H NMR spectra of gel **1** in acetone-d_6, the photodimer solution after 365 nm irradiation for 5 h and the re-formed gel after 254 nm UV illumination for 3 h.

20 (phenyl protons in the periphery of dendron) to 50 (phenyl protons in the periphery of dendron plus phenyl protons in nitrocinnamate moieties), and a new peak of methine protons of cyclobutane at 4.46 ppm appeared. Therefore, it could be estimated that most of the monomeric species were converted to dimer **2**. On the other hand, when the obtained solution was further exposed to UV light at 254 nm, a back-conversion of the proton signals was observed. From ^{13}C NMR spectra, it was seen that the signals of cinnamylidene protons at 144.0 and 118.9 ppm almost disappeared and the signals of the cyclobutane carbons emerged at 44.2 ppm (the peaks indicated by arrow in Fig. S6, Supplementary data). Moreover, the molecular ion peaks of dimeric species appeared after irradiation revealed by MALDI-TOF MS measurement. However, both the molecular ion peaks of monomer and dimer still co-existed after irradiating at 254 nm for a sufficient time (see Supplementary data), which agreed well with the result that the photocleavage reaction of dimers was incomplete as shown from UV–vis and NMR spectra.

In order to ascertain the ratio of monomer and dimer in the original gel, the solution converted from the gel and the re-formed gel, analytical RP HPLC was performed with the wavelength of 309 nm as the characteristic peak and methanol/water (9:1, v/v) as the eluting solvents (Fig. 7). It can be seen that the amount of monomer species decrease to 9% upon UV (λ=365 nm) irradiation. However, it returned to only 35% after further irradiation with UV light (λ=254 nm). Although the presence of a majority of dimers, the monomers still aggregated to fibrous networks, indicating the photocleavage was not complete under these conditions, and the re-formed system in fact was a co-existed state including the gel phase assemblies and the amorphous structures (Fig. 4d).

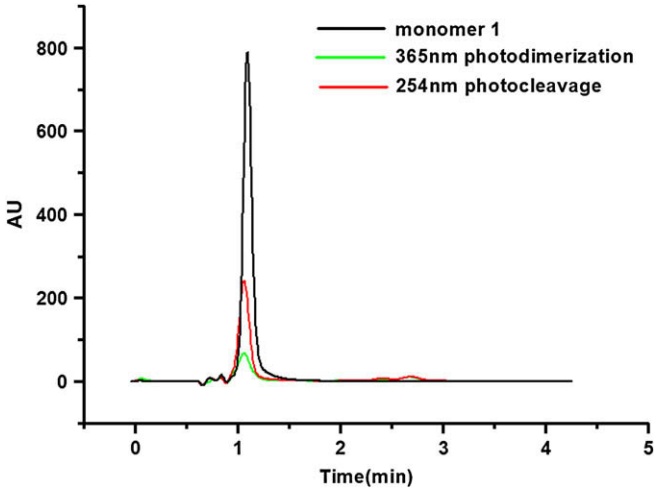

Figure 7. RP HPLC chromatograms of **1** in original, upon 365 nm irradiation and 254 nm irradiation states. Condition: column: ZORBAX Extend-C18 column, 50×2.1 mm i.d., 3.5 μm particle size, flow rate: 0.25 mL/min, mobile phase of methanol/water (9:1, v/v), injection volume: 5 μL, c=6 mg/mL.

3. Conclusions

We have created a new photoresponsive organogel from the amino acid-based dendron **1** functionalized with *p*-nitrocinnamate at the focal point. The sol–gel interconversion in response to external photo-stimuli is attributed to the cycloaddition and cleavage of the focal cinnamate groups. TEM, UV–vis, NMR, MALDI-TOF MS, and RP HPLC monitoring these processes shed some light on the responsive transition. It is expected that smart dendritic gels will potentially have more applications than other LMOGs. The presence of photoactive cinnamate/coumarin moieties in the gelator offers the distinct advantages in the transformation between the gel and sol. Such materials may not only lead to the fabrication of cinnamate-based device but also provide a novel path to design smart materials.

4. Experimental section

4.1. General

Unless stated otherwise, all reagents and common solvents were obtained from commercial sources and used as received. ^{1}H NMR and ^{13}C NMR spectra were recorded on Brucker 400 MHz spectrometer. MALDI-TOF mass-spectra were acquired on a BIFLE XIII time-of-flight MALDI mass spectrometer with α-cyano-4-hydroxycinnamic acid (CCA) as the matrix. FTIR spectra were obtained using a Bruker VECTOR22 IR spectrometer. TEM was applied by a JEM-100 CXII microscope, operating at an acceleration voltage of 100 kV. Powder wide-angle X-ray diffraction (WAXD) patterns of the xerogels were obtained using a Bruker D8 Discover diffractometer with GADDS as a 2D detector. Air scattering was subtracted from the sample patterns. Diffraction patterns were recorded in a transmission mode at room temperature employing Cu Kα radiation. Gel was naturally dried for two days at room temperature before WAXD experiment. UV irradiation (365 nm) was performed by using a high-pressure lamp from the Techcomp Limited Co. LTD. UV irradiation (254 nm) was utilized a low-pressure lamp provided by Beijing Aerospace HONGDA Optoelectronics Technology Co., LTD. RP HPLC utilized Agilent 1100 series HPLC system (Agilent Technologies, Palo Alto, CA, USA) equipped with an autosampler and diode-array detector. *Condition*: column: ZORBAX Extend-C18 column, 50×2.1 mm i.d., 3.5 μm particle size, flow rate: 0.25 mL/min,

mobile phase of methanol/water (9:1, v/v), injection volume: 5 μL, c=6 mg/mL.

4.2. Synthesis of 1

A mixture of *p*-nitrocinnamate acid (0.11 g, 0.57 mmol) and $SOCl_2$ (25 mL) was heated to reflux for 3 h. The solvent was evaporated under reduced pressure. CH_2Cl_2 (5 mL) was added and evaporated again. A $CHCl_3$ (2 mL) solution of the resultant was added dropwise to a $CHCl_3$ solution of TFA·NH_2-G2[26] (0.2 g, 0.19 mmol) and triethylamine (0.5 mL) under N_2. After the reaction mixture was stirred for 24 h, the solvent was evaporated. The residue was dissolved in a small amount of mixed solvents (1:9 $CH_3OH/CHCl_3$), and the precipitate were formed in cold diethyl ether, filtered, and dried. The crude product was precipitated by diethyl ether again and subjected to column chromatography (SiO_2: $CHCl_3$/MeOH 15:1). Yield: 62%. ^{1}H NMR (400 MHz, DMSO-d_6, rt, TMS) ppm: 8.50–8.49 (d, 2H, NO_2–Ar–H), 8.48–8.23 (m, 6H, NHCO), 7.60–7.40 (d, 0.7H, C*H*═C*H*–Ar–H), 7.40–7.20 (s, 20H, CH_2–Ar–*H*), 7.00–6.90 (d, 0.6H, C*H*═CH–Ar), 6.80–6.60 (d, 0.4H, CH═C*H*–Ar), 6.30–6.20 (d, 0.3H, CH═C*H*–Ar), 5.09–5.05 (m, 8H, CO$CH_2C_6H_5$), 4.79–4.75 (m, 2H, NHCHCO), 3.92–3.91 (m, 2H, NHCH_2CO), 3.77–3.71 (m, 4H, $NHCH_2CO$), 2.91–2.80 (m, 5H, $CHCH_2CO$). ^{13}C NMR (100 MHz, rt, DMSO-d_6) ppm: 171.16–168.84 (CH_2CO), 164.68 (CH═CH–*C*ONH), 147.54 (NO_2–Ar–*C*), 118.51 (CH═*C*H–Ar), 144.01 (CH═CH–Ar–*C*), 135.70–135.82, ($CH_2C_6H_5$), 128.15–128.56 ($CH_2C_6H_5$), 66.74–65.92 ($OCH_2C_6H_5$), 49.91–48.62 ($NHCH_2CO$), 41.99–41.83 ($NHCH_2CO$), 35.78 ($CHCH_2CO$). MALDI-TOF MS: $C_{55}H_{55}N_7O_{16}$ m/z calcd 1069; found [M+Na]: 1092, [M+K]: 1108. Elemental Anal. C, 61.73% (found 61.36%); H, 5.18% (found 5.09); N, 9.16% (found 9.03%).

Acknowledgements

The authors would like to thank the National Natural Science Foundation of China (NSFC No. 20774003) and National Basic Research Program of China (973 Program, 2007CB935800–2007CB935801) for the financial support.

Supplementary data

Supplementary data associated with this article can be found in the online version, at doi:10.1016/j.tet.2009.02.038.

References and notes

1. Ahmed, S. A.; Sallenave, X.; Fages, F.; Mieden-Gundert, G.; Müller, W. M.; Müller, U.; Vogtle, F.; Pozzo, J. L. *Langmuir* **2002**, *18*, 7096–7101.
2. Moon, K. S.; Kim, H. J.; Lee, E.; Lee, M. *Angew. Chem., Int. Ed.* **2007**, *46*, 6807–6810.
3. Pozzo, J. L.; Clavier, G. M.; Desvergne, J. P. *J. Mater. Chem.* **1998**, *8*, 2575–2577.
4. Kim, H. J.; Lee, J. H.; Lee, M. *Angew. Chem., Int. Ed.* **2005**, *44*, 5810–5814.
5. (a) Kawano, S. I.; Fujita, N.; Shinkai, S. *J. Am. Chem. Soc.* **2004**, *126*, 8592–8593; (b) Tsuchiya, K.; Orihara, Y.; Kondo, Y.; Yoshino, N.; Ohkubo, T.; Sakai, H.; Abe, M. *J. Am. Chem. Soc.* **2004**, *126*, 12282–12283.
6. (a) Paulusse, J. M. J.; Sijbesma, R. P. *Angew. Chem., Int. Ed.* **2006**, *45*, 2334–2337; (b) Naota, T.; Koori, H. *J. Am. Chem. Soc.* **2005**, *127*, 9324–9325; (c) Isozaki, K.; Takaya, H.; Naota, T. *Angew. Chem., Int. Ed.* **2007**, *46*, 2855–2857.
7. (a) Murata, K.; Aoki, M.; Suzuki, T.; Harada, T.; Kawabata, H.; Komori, T.; Ohseto, F.; Ueda, K.; Shinkai, S. *J. Am. Chem. Soc.* **1994**, *116*, 6664–6676; (b) Koumura, N.; Kudo, M.; Tamaoki, N. *Langmuir* **2004**, *20*, 9897–9900; (c) Yagai, S.; Nakajima, T.; Kishikawa, K.; Kohmoto, S.; Karatsu, T.; Kitamura, A. *J. Am. Chem. Soc.* **2005**, *127*, 11134–11139; (d) Yagai, S.; Nakajima, T.; Karatsu, T.; Saitow, K.; Kitamura, A. *J. Am. Chem. Soc.* **2004**, *126*, 11500–11508; (e) Zhou, Y. F.; Xu, M.; Yi, T.; Xiao, S. Z.; Zhou, Z. G.; Li, F. Y.; Huang, C. H. *Langmuir* **2007**, *23*, 202–208; (f) Yagai, S.; Karatsu, T.; Kitamura, A. *Chem.—Eur. J.* **2005**, *11*, 4054–4063; (g) Matsuzawa, Y.; Ueki, K.; Yoshida, M.; Tamaoki, N.; Nakamura, T.; Sakai, H.; Abe, M. *Adv. Funct. Mater.* **2007**, *17*, 1507–1514.
8. Eastoe, J.; Sanchez-Dominguez, M.; Wyatt, P.; Heenan, R. K. *Chem. Commun.* **2004**, 2608–2609.
9. (a) de Jong, J. J. D.; N.Lucas, I.; Kellogg, R. M.; van Esch, J. H.; Feringa, B. L. *Science* **2004**, *304*, 278–281; (b) de Jong, J. J. D.; Hania, P. R.; Pugzlys, A.; Lucas, L. N.; de Loos, M.; Kellogg, R. M.; Feringa, B. L.; Duppen, K.; van Esch, J. H. *Angew. Chem., Int. Ed.* **2005**, *44*, 2373–2376; (c) Wang, S.; Shen, W.; Feng, Y. L.; Tian, H. *Chem. Commun.* **2006**, 1497–1499.
10. Kumar, N. S. S.; Varghese, S.; Narayan, G.; Das, S. *Angew. Chem., Int. Ed.* **2006**, *45*, 6317–6321.
11. Frkanec, L.; Jokic, M.; Makarevic, J.; Wolsperger, K.; Zinic, M. *J. Am. Chem. Soc.* **2002**, *124*, 9716–9717.
12. Iwaura, R.; Shimizu, T. *Angew. Chem., Int. Ed.* **2006**, *45*, 4601–4604.
13. (a) Ayabe, M.; Kishida, T.; Fujita, N.; Sada, K.; Shinkai, S. *Org. Biomol. Chem.* **2003**, *1*, 2744–2747; (b) Wang, C.; Zhang, D. Q.; Xiang, J. F.; Zhu, D. B. *Langmuir* **2007**, *23*, 9195–9200.
14. Ji, Y.; Kuang, G. C.; Jia, X. R.; Chen, E. Q.; Wang, B. B.; Li, W. S.; Wei, Y.; Lei, J. *Chem. Commun.* **2007**, 4233–4235.
15. Trenor, S. R.; Shultz, A. R.; Love, B. J.; Long, T. E. *Chem. Rev.* **2004**, *104*, 3059–3078.
16. Ichimura, K.; Akita, Y.; Akiyama, H.; Kudo, K.; Hayashi, Y. *Macromolecules* **1997**, *30*, 903–911.
17. (a) Trivedi, D. R.; Dastidar, P. *Chem. Mater.* **2006**, *18*, 1470–1478; (b) Trivedi, D. R.; Ballabh, A.; Dastidar, P.; Ganguly, B. *Chem.—Eur. J.* **2004**, *10*, 5311–5322.
18. Yu, H. T.; Mizufune, H.; Uenaka, K.; Moritoki, T.; Koshima, H. *Tetrahedron* **2005**, *61*, 8932–8938.
19. (a) Asfura, K. M. G.; Weisman, E.; Andreopoulos, F. M.; Micic, M.; Muller, B.; Sirpal, S.; Pham, S. M.; Leblanc, R. M. *Biomacromolecules* **2005**, *6*, 1503–1509; (b) Micic, M.; Zheng, Y. J.; Moy, V.; Zhang, X. H.; Andreopoulos, F. M.; Leblanc, R. M. *Colloids Surf., B* **2002**, *27*, 147–158; (c) Andreopoulos, F. M.; Beckman, E. J.; Russell, A. J. *J. Polym. Sci., Part A: Polym. Chem.* **2000**, *38*, 1466–1476.
20. Yang, X. C.; Lu, R.; Xu, T. H.; Xue, P. C.; Liu, X. L.; Zhao, Y. *Chem. Commun.* **2008**, 453–455.
21. Lee, S. J.; Lee, S. S.; Kim, J. S.; Lee, J. Y.; Jung, J. H. *Chem. Mater.* **2005**, *17*, 6517–6520.
22. Jang, W. D.; Dong, D. L.; Aida, T. *J. Am. Chem. Soc.* **2000**, *122*, 3232–3233.
23. Xu, L. P.; Yan, C. J.; Wan, L. J.; Jiang, S. G.; Liu, M. H. *J. Phys. Chem. B* **2005**, *109*, 14773–14778.
24. Lee, S. W.; Kim, S. I.; Lee, B.; Choi, W.; Chae, B.; Kim, S. B.; Ree, M. *Macromolecules* **2003**, *36*, 6527–6536.
25. Jiang, J.; Qi, B.; Lepage, M.; Zhao, Y. *Macromolecules* **2007**, *40*, 790–792.
26. Ji, Y.; Luo, Y. F.; Jia, X. R.; Chen, E. Q.; Huang, Y.; Ye, C.; Wang, B. B.; Zhou, Q. F.; Wei, Y. *Angew. Chem., Int. Ed.* **2005**, *44*, 6025–6029.